

Structural and electronic properties of the Pb/Ge(111)- $\beta(\sqrt{3} \times \sqrt{3})R30^\circ$ surface studied by photoelectron spectroscopy and first-principles calculations

Koichiro Yaji*

Institute for Solid State Physics, The University of Tokyo, 5-1-5 Kashiwanoha, Kashiwa-shi, Chiba 277-8581, Japan and JST CREST, Saitama, 332-0012, Japan

Shinichiro Hatta and Tetsuya Aruga†

Department of Chemistry, Graduate School of Science, Kyoto University, Kyoto 606-8502, Japan and JST CREST, Saitama, 332-0012, Japan

Hiroshi Okuyama

Department of Chemistry, Graduate School of Science, Kyoto University, Kyoto 606-8502, Japan

(Received 3 November 2012; published 28 December 2012)

We have studied structural and electronic properties of a Ge(111) surface covered with a monatomic Pb layer [Pb/Ge(111)- β] by means of core-level photoelectron spectroscopy, angle-resolved photoelectron spectroscopy (ARPES), and a first-principles band structure calculation. There has been a controversy about the surface structure of Pb/Ge(111)- β between a close-packed model with a coverage of 4/3 monolayers and a trimer model with a coverage of 1 monolayer. This problem has been examined by analyzing the line shape of a Pb 5*d* core-level spectrum and comparing the experimental band structure with those calculated for two models. The line shape of the core-level spectrum agrees with a close-packed model. The valence band structure observed by ARPES has been well reproduced by the calculation employing the close-packed model. The close-packed model therefore describes correctly the surface structure of Pb/Ge(111)- β . The scanning-tunneling microscopy (STM) image simulated for the close-packed model is in good agreement with the experimental filled-state STM image, in which three protrusions per unit cell were observed.

DOI: [10.1103/PhysRevB.86.235317](https://doi.org/10.1103/PhysRevB.86.235317)

PACS number(s): 73.20.At, 71.70.-d

I. INTRODUCTION

Silicon and germanium surfaces covered with a monatomic layer of *p*-block metals have widely been studied because of their various structural and electronic properties. In some cases, adsorbate-induced surface-state bands cross the Fermi level (E_F) inside a projected bulk band gap giving rise to ultrathin two-dimensional metals.¹⁻⁴ Metallic surface states sometimes cause phase transitions due to the Fermi surface instability at low temperatures.⁵⁻⁷ There is also a possibility that the metallic surface-state bands split into two due to the surface Rashba effect,^{8,9} when spin-orbit interaction is not negligible.¹⁰⁻¹³ A well-known example is a Ge(111) surface covered with a monatomic Pb layer [Pb/Ge(111)- β]. Recently we have reported that the Pb/Ge(111)- β surface has a metallic surface-state band with a Rashba spin splitting of 200 meV at the Fermi wave vector,¹⁴ which indicated that this surface serves as a prototype for the surface spin transport study.

The surface structure of the Pb/Ge(111) system depends on Pb coverage. There are two different ($\sqrt{3} \times \sqrt{3}$) $R30^\circ$ structures at room temperature (RT): The dilute (dense) phase is called the α (β) phase. The coverage of Pb/Ge(111)- α is 1/3 monolayer, in which a Pb atom occupies a T_4 site in the ($\sqrt{3} \times \sqrt{3}$) $R30^\circ$ unit cell at RT.¹⁵ On the other hand, for the dense phase Pb/Ge(111)- β , there remains a controversy between a close-packed model with a coverage of 4/3 monolayers¹⁶⁻²⁶ and a trimer model with a coverage of 1 monolayer,²⁷⁻³⁰ which are shown in Fig. 1. For the close-packed model, one Pb atom is located at an H_3

site and three Pb atoms are located at the off-centered (OC) bridge position between T_1 and T_4 sites as shown in Fig. 1(a). On the other hand, for the trimer model, three Pb atoms form a trimer centered at the H_3 site as shown in Fig. 1(b).

In the present paper we report on the structural and electronic properties of Pb/Ge(111)- β investigated by core-level spectroscopy, angle-resolved photoelectron spectroscopy (ARPES), and a first-principles electronic band structure calculation. We show that the Pb 5*d* core-level spectrum as well as the comparison of the experimental and computed band structures support the close-packed model. The character of the surface-state bands of Pb/Ge(111)- β is discussed. We have also simulated the scanning-tunneling microscopy (STM) image of the Pb/Ge(111)- β surface on the basis of the close-packed model. The simulated image is in good agreement with the experimental STM image,³⁰ which appears to favor the trimer model.

II. EXPERIMENT AND CALCULATION METHODS

Experiments were performed in an ultrahigh-vacuum system with a base pressure lower than 2.0×10^{-10} Torr. An *n*-type Ge(111) substrate was prepared by several cycles of 0.7 keV Ar⁺ sputtering and subsequent annealing up to 900 K for a minute, which gave a good $c(2 \times 8)$ low-energy electron diffraction (LEED) pattern. Pb was then deposited onto the surface kept at RT from an alumina crucible heated with a tungsten filament. The surface after the Pb deposition was annealed at 570 K for 5 min.

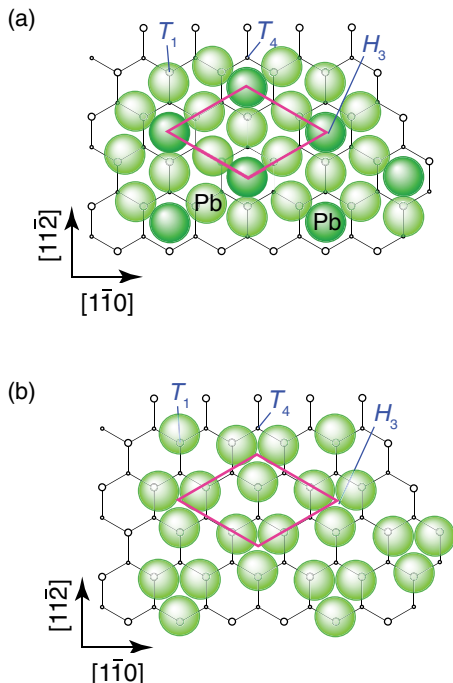


FIG. 1. (Color online) Schematic illustration of the surface structure models for Pb/Ge(111)- β ($\sqrt{3}\times\sqrt{3}$) $R30^\circ$: (a) Close-packed model with a coverage of $4/3$ monolayers and (b) trimer model with a coverage of 1 monolayer. The large and small circles denote the Pb adatoms and Ge atoms in the topmost layer, respectively. The thin solid lines represent the bonds between the Ge atoms. The solid parallelograms represent the unit cell of the ($\sqrt{3}\times\sqrt{3}$) $R30^\circ$ periodicity.

The core-level photoelectron spectra were measured at normal emission using monochromatic He II ($h\nu = 40.82$ eV) radiation. In the ARPES measurements, monochromatic He I α ($h\nu = 21.22$ eV) radiation was used and the energy and angular resolutions were 10 meV and 0.4° , respectively. The sample temperature was maintained at 30 K during the ARPES measurement. Note that the Pb/Ge(111)- β surface exhibits no structural phase transition down to 6 K.³⁰ All the measurements were finished in 10 h after the surface was prepared. We confirmed that the sharp and low-background LEED pattern was observed after the ARPES measurement. Energy band dispersion as a function of the wave vector parallel to the surface (k_{\parallel}) was obtained from the ARPES spectra using the formula $k_{\parallel} = \sin\theta\sqrt{2m_e}(h\nu - E_B - \Phi)/\hbar$, where E_B denotes the binding energy, Φ is the work function of the sample, and θ is the photoelectron emission angle. The work function was determined from the cut-off energy of secondary electrons.

The first-principles calculation has been performed using the WIEN2K computer code based on the “augmented plane wave + local orbitals” (APW + lo) method with the spin-orbit interaction taken into account.^{31–34} The surface was modeled by a 24-layer Ge(111) slab with one side covered with a β -($\sqrt{3}\times\sqrt{3}$) $R30^\circ$ -Pb layer and the opposite side terminated by hydrogen atoms. The atomic positions were optimized until the root mean square of the forces exerted on the atoms become negligibly small (<2 mRy/a.u.).

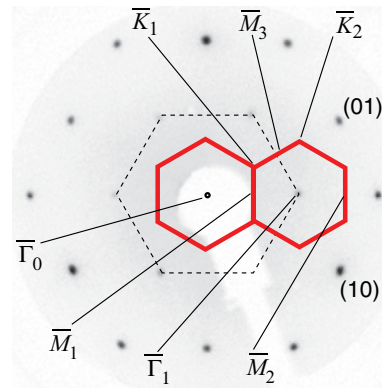


FIG. 2. (Color online) LEED pattern of Pb/Ge(111)- β together with the surface Brillouin zones (SBZ). The primary electron energy was 55 eV. The dashed and solid lines denote the (1×1) and ($\sqrt{3}\times\sqrt{3}$) $R30^\circ$ SBZ, respectively.

III. RESULTS AND DISCUSSION

A. Pb $5d$ core-level spectroscopy

The amount of deposited Pb was optimized by monitoring the width of the Pb $5d_{5/2}$ core-level spectra³⁵ and the spot sharpness and background intensity of the LEED pattern. The obtained surface gave a sharp and low-background ($\sqrt{3}\times\sqrt{3}$) $R30^\circ$ LEED pattern as shown in Fig. 2. The high-resolution Pb $5d_{5/2}$ core-level spectrum for the carefully prepared Pb/Ge(111)- β surface is shown by open circles in Fig. 3, which exhibits a main peak at 17.8 eV below E_F and a shoulder at the higher binding-energy side. We have confirmed that the line shape of the core-level spectrum is unchanged in the temperature range of 30–300 K except for moderate thermal broadening. In addition, the core-level spectrum shows an asymmetric line shape with a tail toward the high-binding-energy side, which reflects a metallic screening effect of the core-level excitation process.

The core-level spectrum was analyzed by using the Doniach-Šunjić (DS) function convoluted with a Gaussian function, where the DS function has been defined as the one-sided power-law function convoluted with a Lorentzian function.^{36–38} In the fitting procedure, the full width at half

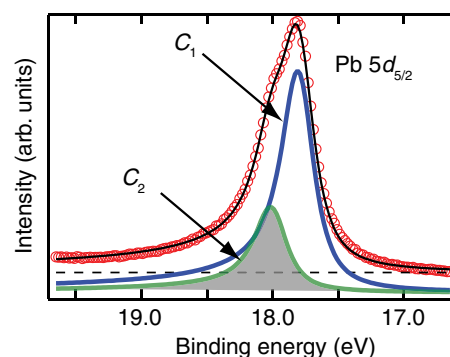


FIG. 3. (Color online) Pb $5d_{5/2}$ core-level spectrum for Pb/Ge(111)- β . The core-level spectrum is fitted by the DS function convoluted with a Gaussian. Best fitting result is shown by a thin solid curve. The spectrum is reproduced by the summation of the two components shown by bold solid (blue and green) curves (C_1 and C_2).

maximum (FWHM) of the Lorentzian function was fixed at 0.20 eV and the singularity index of the DS function was optimized to be 0.13.³⁹ The fitting parameters are thus the peak positions, the intensities, and the FWHM of the Gaussian function.

The Pb $5d_{5/2}$ spectrum was well fitted by the summation of the two components (C_1 and C_2) as shown by the solid curve in Fig. 3. The peak of component C_1 is found at 17.80 eV, while the other component C_2 is located at a 0.20 eV high binding energy. The spectrum was well fitted with a Gaussian width of 0.13 eV for both the C_1 and C_2 components. The existence of two components indicates that there are Pb atoms in two inequivalent environments on the Pb/Ge(111)- β surface. The intensity ratio between C_1 and C_2 is determined to be 2.6:1. The result is inconsistent with the trimer model, which predicts that all the Pb atoms are equivalent. The close-packed model consists of three Pb atoms at the OC bridge position and one at the H_3 site, which is in good accordance with the intensity ratio of C_1 and C_2 . Therefore we conclude that the core-level spectrum is consistent with the close-packed model with the C_1 and C_2 components corresponding to Pb atoms located at the OC bridge and H_3 site, respectively.

B. Valence band structure observed by ARPES

Figure 4 shows the ARPES images of the Pb/Ge(111)- β surface measured along two symmetry axes $\bar{\Gamma}\bar{M}$ and $\bar{\Gamma}\bar{K}\bar{M}\bar{K}$ (see Fig. 2.) of the $(\sqrt{3}\times\sqrt{3})R30^\circ$ surface Brillouin zone (SBZ). In both directions, the characteristic Pb-induced surface-state bands are clearly observed within 2 eV below E_F . These high-resolution ARPES data provide a significant information of the surface-state bands for Pb/Ge(111)- β compared with those reported in the former studies.^{30,35,40}

For the valence band structure along $\bar{\Gamma}\bar{M}$ shown in Fig. 4(a), three Pb-induced bands labeled S_1 , S_2 , and S_3 are observed.

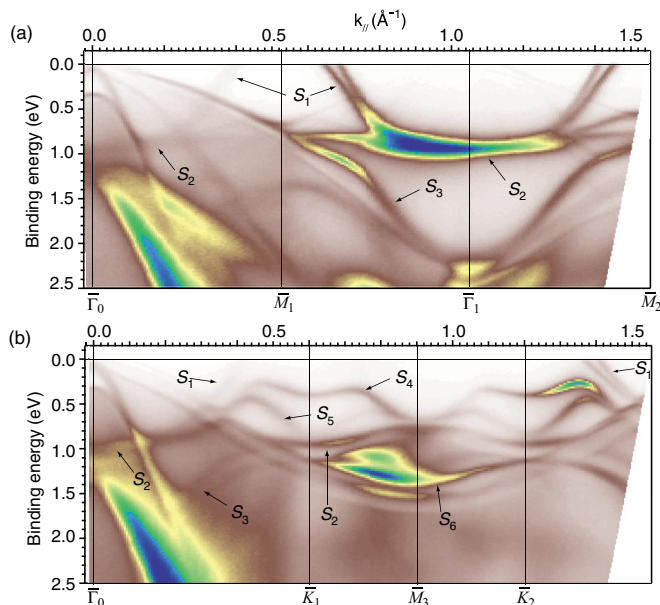


FIG. 4. (Color online) Experimental energy band dispersion of Pb/Ge(111)- β along (a) $\bar{\Gamma}\bar{M}$ and (b) $\bar{\Gamma}\bar{K}\bar{M}\bar{K}$ of the $(\sqrt{3}\times\sqrt{3})R30^\circ$ SBZ. The Pb-induced bands are denoted as S_1 – S_6 .

The S_1 band exhibits a steep dispersion, crosses the Fermi level in the projected bulk band gap, and is clearly split into two. This splitting is due to the Rashba effect, which was confirmed by means of spin-resolved ARPES.¹⁴ The S_2 and S_3 bands appear in the projection of Ge bulk bands and hence are surface resonances. The overall dispersion of S_1 , S_2 , and S_3 suggests that a free-electron-like parabolic band, the bottom of which is located below 2.0 eV, is hybridized with a nearly flat band at ~ 0.9 eV (S_2), yielding upper (S_1) and lower (S_3) branches. Several bands steeply disperse downward from the $\bar{\Gamma}_0$ point. Intense feature with an energy maximum 1.2–1.3 eV at $\bar{\Gamma}_0$ is attributed to direct transitions between bulk bands.⁴¹ Some of the bands near the valence band maximum (VBM) around $\bar{\Gamma}_0$ may be ascribed to the Ge-derived surface states and surface resonances. Similar surface bands were observed and analyzed in other adsorption systems such as Bi/Ge(111)¹² and Br/Ge(111).⁴² In the present paper we focus on the Pb-induced surface-state bands, and do not try to describe the details of these Ge-derived surface bands.

In Fig. 4(b) the ARPES image along the $\bar{\Gamma}\bar{K}\bar{M}\bar{K}$ direction is shown. The spin-split S_1 band is observed also in the $\bar{\Gamma}\bar{K}\bar{M}\bar{K}$ direction. The S_2 band lying in the energy range of 0.7–1.0 eV below E_F can also be recognized. The S_4 and S_5 bands dispersing in the energy range 0.2–0.9 eV exhibit a semiconducting behavior. The S_6 surface resonance band, which exhibits strong intensity at around $\bar{K}_1\bar{M}_3\bar{K}_2$, appears to disperse in parallel with the edge of the bulk heavy-hole band. Several Ge-derived bands are also observed around $\bar{\Gamma}_0$.

C. Electronic property and surface-structure model

Comparison between the experimental and calculated band structures allows us to identify the correct structure model. In Fig. 5 we show the calculated band structures of Pb/Ge(111)- β with the close-packed and the trimer models. In the calculation for each model, the surface structure has been optimized by minimizing the total energy. The energy relative to VBM is plotted. The radii of circles are proportional to the contribution of Pb $6p_x$, and the color index represents the relative contribution of Pb $6p_x p_y$ and $6p_z$, where the z axis is normal to the surface.

The calculated bands for the two models are significantly different. For instance, while the metallic band along $\bar{\Gamma}\bar{M}$ is observed for both models, the parabolic band with its bottom at ~ 2 eV is observed only for the close-packed model. The band structure at 0.5–1.2 eV along $\bar{\Gamma}\bar{M}$ is also considerably different for both models. For $\bar{\Gamma}\bar{K}\bar{M}\bar{K}$, the difference is also significant: While a metallic band is observed between $\bar{\Gamma}$ and \bar{K} for the close-packed model, an electron pocket is formed around \bar{K} for the trimer model.

Comparing these results with the experimental band structure (4), it is evident that the band structure calculated for the close-packed model is consistent with the experiment. In the $\bar{\Gamma}\bar{M}$ direction shown in Fig. 5(a), the Pb-derived bands S_{1C} , S_{2C} , S_{3C} , and U_{1C} are found. The calculated S_{1C} band, which shows the rapid parabolic dispersion with the Rashba spin splitting, well agrees with the experimental S_1 band shown in Fig. 4(a). The S_{2C} band slightly disperses in the energy range of 0.5–0.7 eV along $\bar{\Gamma}\bar{M}$. The overall feature of the calculated S_{2C} band well reproduces the experimental results.

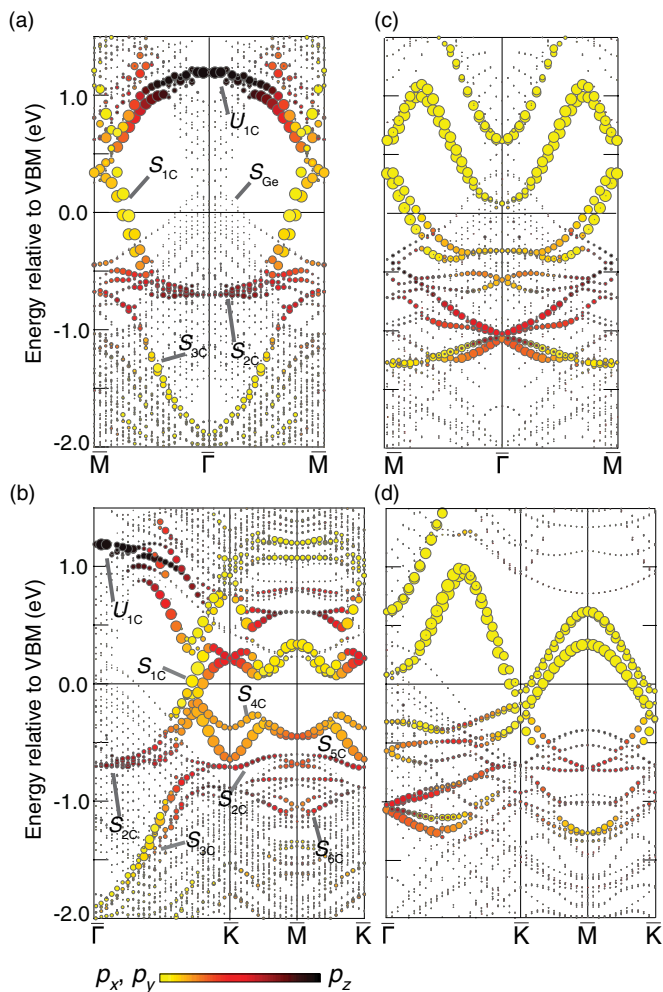


FIG. 5. (Color online) Calculated band structure for the close-packed model along (a) $\bar{\Gamma}\bar{M}\bar{\Gamma}$ and (b) $\bar{\Gamma}\bar{K}\bar{M}\bar{K}$, and for the trimer model along (c) $\bar{\Gamma}\bar{M}\bar{\Gamma}$ and (d) $\bar{\Gamma}\bar{K}\bar{M}\bar{K}$. The size of the circles are proportional to the net contribution of Pb $6p$. The relative contribution of Pb $6p_x p_y$ and $6p_z$ are shown by color scale.

The X-shaped bands at $\bar{\Gamma}$ in the calculation for the trimer model [5(c)] is not observed in the ARPES result. The S_{3C} band shows the energy minimum at ~ 2 eV below VBM at the $\bar{\Gamma}$ point and disperses upward, which also agrees with the experiment shown in Fig. 4(a).

The calculated band structure for the close-packed model along $\bar{\Gamma}\bar{K}\bar{M}\bar{K}$ [5(b)] is also in accordance with the ARPES result shown in Fig. 4(b). In particular, the semiconducting behavior of the S_4 and S_5 bands are well reproduced, while the trimer model predicts metallic bands along $\bar{K}\bar{M}$.

The calculated band structure for the close-packed model contains the information of unoccupied states. The unoccupied band U_{1C} is found at 0.5–1.2 eV above VBM [Figs. 5(a) and 5(b)]. The U_{1C} band has a strong Pb $6p_z$ contribution and shows a maximum at 1.2 eV above VBM at the $\bar{\Gamma}$ point and disperses downward.

We next describe the character of the surface-state bands. The metallic spin-split S_{1C} band is predominantly of Pb $6p_x p_y$ character except for the region near the \bar{K} point as found in Figs. 5(a) and 5(b). This is more clearly observed in the

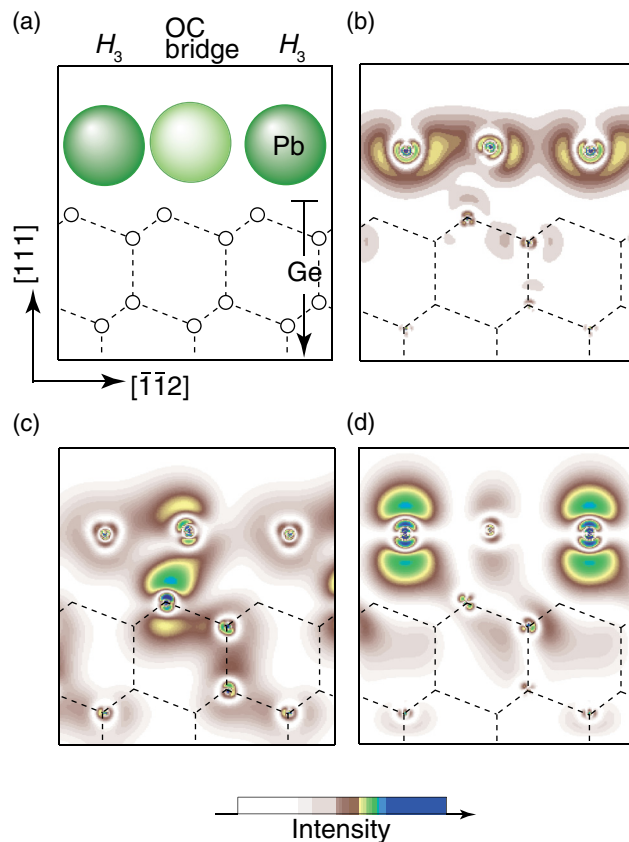


FIG. 6. (Color online) (a) Schematic drawing of Pb/Ge(111)- β in $(\bar{1}10)$ plane. The large and small circles denote the Pb adatoms and Ge atoms, respectively. Dashed lines represent the lattice of the Ge(111) substrate. (b)–(d) Charge density distribution of the (b) S_{1C} , (c) S_{2C} , and (d) U_{1C} states in the $(\bar{1}10)$ plane.

charge density plot of the S_{1C} state near E_F as shown in Fig. 6(b), which indicates that the wave function is of in-plane p character and is highly localized in the Pb monolayer.

The S_{2C} and U_{1C} bands have Pb $6p_z$ character. The charge distribution shown in Fig. 6(c) clearly indicates that the S_{2C} band is actually a bonding state between the dangling bond ($4p_z$) of topmost Ge atoms and $6p_z$ of Pb atoms at the OC bridge sites. Note that the $6p_z$ wave function in the vacuum side is tilted toward the H_3 site. On the other hand, the U_{1C} band is of antibonding character with respect to Ge-Pb bonds as indicated by the node between Ge and OC-bridge Pb atoms. The wave function of the U_{1C} band is composed largely of $6p_z$ of H_3 Pb atoms.

The Pb atoms in the H_3 sites exhibit negligible bonding interaction with the Ge substrate. It is the delocalized σ bonding by $6p_x p_y$ orbitals that stabilizes the H_3 Pb atoms in the Pb monolayer.

The S_{3C} band is also of in-plane Pb $6p_x p_y$ character, but is significantly mixed with the Ge bulk states. The S_{4C} and S_{5C} bands are also mainly of the in-plane Pb $6p_x p_y$ character. Concerning the S_{6C} band, the Pb $6p_x p_y$ character is included but the Ge contribution is much larger.

In Fig. 7 we show a filled-state STM image simulated for the close-packed structure, which was generated by integrating the local density of states for 0–1.0 eV below

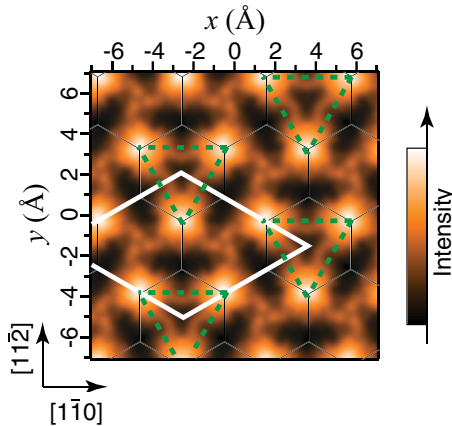


FIG. 7. (Color online) Simulated filled-state STM image ($14 \times 14 \text{ \AA}^2$) of Pb/Ge(111)- β . The thin solid lines represent the bonds between the Ge atoms. The bold solid parallelogram shows the unit cell of $(\sqrt{3} \times \sqrt{3})R30^\circ$. The bold dashed triangles indicate the arrays of trimerlike protrusions.

VBM.⁴³ The simulated STM image should be compared with the experimental STM image.³⁰ The bright protrusions in the simulated STM image form a trimerlike superstructure in the unit cell of $(\sqrt{3} \times \sqrt{3})R30^\circ$. This simulated image is quite similar to the experimental STM image with the positive tip bias 1.0 V.³⁰ Remarkably, only three Pb atoms are found in the unit cell of $(\sqrt{3} \times \sqrt{3})R30^\circ$ and the Pb atom at H_3 does not appear, despite the fact that the four Pb atoms are lying on the topmost Ge layer at nearly the same height. In addition, the bright protrusions are located close to the T_1 sites, which deviate from the actual positions of the OC bridge Pb atoms obtained from the x-ray diffraction.²⁵ The characteristics of the STM image are explained by the charge density distribution shown in Fig. 6. The S_{2C} state, which has the Pb $6p_z$ character and has a large amplitude at the OC bridge Pb atoms, is mainly detected in the experimental STM observation with the positive tip bias 1.0 V. Since the S_{2C} state has a very small amplitude at the H_3 Pb atoms, only the OC bridge Pb atoms are visible at positive tip bias. Note also that the wave function of the S_{2C} state in the vacuum side is tilted toward the H_3 site

in Fig. 6(c), which is in accordance with the STM observation of protrusions near the H_3 sites.

The calculated band structure suggests that four Pb atoms in the unit cell of $(\sqrt{3} \times \sqrt{3})R30^\circ$ should be observed by STM at a very low bias voltage since only the S_{1C} state should contribute to the STM image and the S_{1C} state has an amplitude both at H_3 and OC bridge Pb atoms. This is in agreement with a previous experiment.²² On the other hand, the empty-state STM image with the sample bias of +2 V exhibited bright protrusions centered at the H_3 site.²⁹ In this case, the STM image should mainly reflect the unfilled U_{1C} state which has the Pb $6p_z$ character and is strongly localized at H_3 as shown in Fig. 6(d), in good agreement with the observation.

IV. CONCLUSION

We have studied structural and electronic properties of Pb/Ge(111)- β by core-level spectroscopy, ARPES, and first-principles calculations. The result of the Pb $5d_{5/2}$ core-level spectroscopy supports the close-packed model with a coverage of 4/3 monolayers for the surface structure of Pb/Ge(111)- β because the spectrum was well fitted by the two components with intensity ratio $\sim 3:1$. We have presented a band structure of Pb/Ge(111)- β along two main symmetry axes observed by ARPES, in which several Pb-induced surface-state bands have been clearly observed. A metallic surface-state band S_1 shows a large Rashba spin splitting of 200 meV at the Fermi wave vector. The experimental valence band structure has been well reproduced by the first-principles calculation employing the close-packed model with a coverage of 4/3 monolayers. The valence band analysis, therefore, also indicates that the surface structure of Pb/Ge(111)- β is well described by the close-packed model. In addition, we have shown that the STM image simulated for the close-packed model agrees with the reported STM images.^{29,30}

ACKNOWLEDGMENTS

The authors thank Y. Ohtsubo for his support. This work was partly performed at BL-18A and 19A, KEK Photon Factory, Japan (PF-PAC Grant No. 2011G085).

*yaji@issp.u-tokyo.ac.jp

†aruga@kuchem.kyoto-u.ac.jp

¹T. Abukawa, M. Sasaki, F. Hisamatsu, T. Goto, T. Kinoshita, A. Kakizaki, and S. Kono, *Surf. Sci.* **325**, 33 (1995).

²J. N. Crain, A. Kirakosian, K. N. Altmann, C. Bromberger, S. C. Erwin, J. L. McChesney, J.-L. Lin, and F. J. Himpsel, *Phys. Rev. Lett.* **90**, 176805 (2003).

³E. Rotenberg, H. Koh, K. Rosnagel, H. W. Yeom, J. Schäfer, B. Krenzer, M. P. Rocha, and S. D. Kevan, *Phys. Rev. Lett.* **91**, 246404 (2003).

⁴K. Nakatsuji, R. Niihara, Y. Shibata, M. Yamada, T. Iimori, and F. Komori, *Phys. Rev. B* **80**, 081406(R) (2009).

⁵H. W. Yeom, S. Takeda, E. Rotenberg, I. Matsuda, K. Horikoshi, J. Schaefer, C. M. Lee, S. D. Kevan, T. Ohta, T. Nagao, and S. Hasegawa, *Phys. Rev. Lett.* **82**, 4898 (1999).

⁶P. C. Snijders and H. H. Weitering, *Rev. Mod. Phys.* **82**, 307 (2010).

⁷S. Hatta, Y. Ohtsubo, T. Aruga, S. Miyamoto, H. Okuyama, H. Tajiri, and O. Sakata, *Phys. Rev. B* **84**, 245321 (2011).

⁸E. I. Rashba, *Sov. Phys.: Solid State* **2**, 1109 (1960).

⁹Yu. A. Bychkov and E. I. Rashba, *JETP Lett.* **39**, 78 (1984).

¹⁰S. Hatta, T. Aruga, C. Kato, S. Takahashi, H. Okuyama, A. Harasawa, T. Okuda, and T. Kinoshita, *Phys. Rev. B* **77**, 245436 (2008).

¹¹S. Hatta, T. Aruga, Y. Ohtsubo, and H. Okuyama, *Phys. Rev. B* **80**, 113309 (2009).

¹²Y. Ohtsubo, S. Hatta, K. Yaji, H. Okuyama, K. Miyamoto, T. Okuda, A. Kimura, H. Namatame, M. Taniguchi, and T. Aruga, *Phys. Rev. B* **82**, 201307(R) (2010).

¹³Y. Ohtsubo, S. Hatta, H. Okuyama, and T. Aruga, *J. Phys.: Condens. Matter* **24**, 092001 (2011).

- ¹⁴K. Yaji, Y. Ohtsubo, S. Hatta, H. Okuyama, K. Miyamoto, T. Okuda, A. Kimura, H. Namatame, M. Taniguchi, and T. Aruga, *Nat. Commun.* **1**, 17 (2010).
- ¹⁵A. Tejada, R. Cortés, J. Lobo, E. G. Michel, and A. Mascaraque, *J. Phys.: Condens. Matter* **19**, 355008 (2007).
- ¹⁶T. Ichikawa, *Solid State Commun.* **46**, 827 (1983).
- ¹⁷T. Ichikawa, *Solid State Commun.* **49**, 59 (1984).
- ¹⁸R. Feidenhans'l, J. S. Pedersen, M. Nielsen, F. Grey, and R. L. Johnson, *Surf. Sci.* **178**, 927 (1986).
- ¹⁹B. N. Dev, F. Grey, R. L. Johnson, and G. Materlik, *Europhys. Lett.* **6**, 311 (1988).
- ²⁰H. Li and B. P. Tonner, *Surf. Sci.* **193**, 10 (1988).
- ²¹H. Huang, C. M. Wei, H. Li, B. P. Tonner, and S. Y. Tong, *Phys. Rev. Lett.* **62**, 559 (1989).
- ²²L. Seehofer, G. Falkenberg, and R. L. Johnson, *Surf. Sci.* **290**, 15 (1993).
- ²³F. Ancilotto, A. Selloni, and R. Car, *Phys. Rev. Lett.* **71**, 3685 (1993).
- ²⁴G. E. Franklin, M. J. Bedzyk, J. C. Woicik, C. Liu, J. R. Patel, and J. A. Golovchenko, *Phys. Rev. B* **51**, 2440 (1995).
- ²⁵S. A. de Vries, P. Goettkindt, P. Steadman, and E. Vlieg, *Phys. Rev. B* **59**, 13301 (1999).
- ²⁶Y. Ohtsubo, H. Muto, K. Yaji, S. Hatta, H. Okuyama, and T. Aruga, *J. Phys.: Condens. Matter* **23**, 435001 (2011).
- ²⁷J. J. Métois and G. Le Lay, *Surf. Sci.* **133**, 422 (1983).
- ²⁸I.-S. Hwang and J. A. Golovchenko, *Phys. Rev. Lett.* **71**, 255 (1993).
- ²⁹I.-S. Hwang and J. A. Golovchenko, *Phys. Rev. B* **50**, 18535 (1994).
- ³⁰H. Morikawa, I. Matsuda, and S. Hasegawa, *Phys. Rev. B* **77**, 193310 (2008).
- ³¹P. Blaha, K. Schwarz, G. K. H. Madsen, K. Kvasnicka, and J. Luitz, *WIEN2k, an Augmented Plane Wave Plus Local Orbital Program for Calculating Crystal Properties* (Karlheinz Schwarz, Technical Universität Wien, Wien, Austria, 2001).
- ³²K. Schwarz, P. Blaha, and G. K. H. Madsen, *Phys. Commun.* **147**, 71 (2002).
- ³³E. Sjöstedt, L. Nordström, and D. J. Singh, *Solid State Commun.* **114**, 15 (2000).
- ³⁴G. K. H. Madsen, P. Blaha, K. Schwarz, E. Sjöstedt, and L. Nordström, *Phys. Rev. B* **64**, 195134 (2001).
- ³⁵J. A. Carlisle, T. Miller, and T.-C. Chiang, *Phys. Rev. B* **47**, 3790 (1993).
- ³⁶S. Doniach and M. Šunjić, *J. Phys. C* **3**, 285 (1970).
- ³⁷G. K. Wertheim and S. B. Diczio, *J. Electron Spectrosc. Relat. Phenom.* **37**, 57 (1985).
- ³⁸S. Hüfner, *Photoelectron Spectroscopy* (Springer, Berlin, 1994), p. 176.
- ³⁹W. H. Choi, K. S. Kim, and H. W. Yeom, *Phys. Rev. B* **78**, 195425 (2008).
- ⁴⁰B. P. Tonner, H. Li, M. J. Robrecht, M. Onellion, and J. L. Erskine, *Phys. Rev. B* **36**, 989 (1987).
- ⁴¹R. D. Bringans, R. I. G. Uhrberg, and R. Z. Bachrach, *Phys. Rev. B* **34**, 2373 (1986).
- ⁴²Y. Ohtsubo, S. Hatta, N. Kawai, A. Mori, Y. Takeichi, K. Yaji, H. Okuyama, and T. Aruga, *Phys. Rev. B* **86**, 165325 (2012).
- ⁴³J. Tersoff and D. R. Hamann, *Phys. Rev. B* **31**, 805 (1985).